Do Composite Single-Walled Nanotubes Have Enhanced Capability for Lithium Storage?

Zhen Zhou,*[,†,‡] Jijun Zhao,[§] Xueping Gao,[‡] Zhongfang Chen,*[,||] Jie Yan,[‡] Paul von Ragué Schleyer,[||] and Masahiko Morinaga[†]

Department of Materials Science and Engineering, Graduate School of Engineering, Nagoya University, Furo-cho, Chikusa-ku, Nagoya 464-8603, Japan, Institute of New Energy Material Chemistry, Institute of Scientific Computing, Nankai University, Tianjin 300071, China, Department of Physics and Astronomy, University of North Carolina at Chapel Hill, Chapel Hill, North Carolina 27599, and Department of Chemistry and Center for Computational Quantum Chemistry, University of Georgia, Athens, Georgia 30602

Received July 30, 2004. Revised Manuscript Received November 22, 2004

The lithium adsorption energies of C, BC_3, BC_2N, and BN single-walled nanotubes and the electronic structures of the lithium-intercalated nanotubes products were computed using density functional methods. Due to the strong propensity of boron to accept electrons from lithium energetically, the electron-deficient BC_3 nanotubes, both zigzag and armchair, adsorb lithium very favorably. Electron-sufficient BN nanotubes with partial ionic bonding, in contrast, adsorb lithium poorly. In addition, the wide band gap and low electrical conductivity of BN nanotubes make them unsuitable for Li ion battery applications. Hence, Li adsorption depends critically on the electronic structure of composite nanotubes. Also, our study of lithium diffusion in C and BC_3 nanotubes revealed that high energy barriers preclude Li passage through the sidewalls of perfect BC_3 nanotubes. However, the penetration barriers for C nanotubes are twice as large. Model studies also show that it is possible that dilithium can be adsorbed favorably on the exterior of carbon nanotubes, while the BC_3 tubes can adsorb lithium atoms both inside and outside. The present computations suggest that BC_3 nanotubes are promising candidates for Li intercalation materials suitable for battery applications.

1. Introduction

The considerable demand for lithium ion secondary batteries with high energy storage density, useful in the portable electronic products, has spawned many explorations of new lithium intercalation materials with superior performance both as cathodes and as anodes.[1] In Li ion batteries, graphitic carbon anodes are employed instead of metallic Li electrodes because of safety and cycle efficiency considerations.[2] However, graphite is far from being an ideal host material. Its use results in a specific capacity reduction from 3860 mAh/g for metallic Li to 372 mAh/g for graphitic anodes. Carbon nanotubes are expected to exhibit superior Li adsorption capabilities provided that Li ions can intercalate both into the interstitial spaces between the nanotubes and into the nanotube interiors. However, the initial experimental results were somewhat disappointing: both Li intercalated multiwalled (MWNT) and single-walled (SWNT) nanotubes without any posttreatment[3−5] showed only 25% higher reversible capacity than graphite itself. The optimization of nanotubes for the utilization as energy storage materials requires several important issues to be addressed. For example, the diffusion mechanisms and diffusion channels for Li ions and the effects of structural defects on nanotubes are important.[6] Recent experiments have shown that the maximum capacity for SWNTs can be increased up to $Li_{2.7}C_6$ (∼1000 mAh/g) via chemical etching or ball-milling of the nanotubes.[7,8] In these cases, the increase in Li capacity has been attributed to Li intercalation inside the nanotube interior space. Lithium enters the interior of nanotubes either through the opened tube ends or through defects in the tube sidewalls created by chemical etching or ball-milling. Zhao et al. simulated Li intercalation in SWNT bundles and demonstrated the possibility of high saturation density of about Li_3C_6.[9] The doping of alkali metals inside carbon nanotubes has also been studied by many other groups.[10−15] However, much less is known about alkali metal doping in newly

* Corresponding authors. E-mail: shushin@silky.numse.nagoya-u.ac.jp (Z.Z.); chen@chem.uga.edu (Z.C.).
† Nagoya University.
‡ Nankai University.
§ University of North Carolina at Chapel Hill.
|| University of Georgia.

(1) Tarascon, J.-M.; Armand, M. *Nature* **2001**, *414*, 359.
(2) Dahn, J. R.; Zheng, T.; Liu, Y.; Xue, J. S. *Science* **1995**, *270*, 590.
(3) Maurin, G.; Bousquet, Ch.; Henn, F.; Bernier, P.; Almairac, R.; Simon, B. *Chem. Phys. Lett.* **1999**, *312*, 14.
(4) Gao, B.; Kleinhammes, A.; Tang, X. P.; Bower, C.; Fleming, L.; Wu, Y.; Zhou, O. *Chem. Phys. Lett.* **1999**, *307*, 153.
(5) Claye, A. S.; Fischer, J. E.; Huffmann, C. B.; Rinzler, A. G.; Smalley, R. E. *J. Electrochem. Soc.* **2000**, *147*, 2845.
(6) Meunier, V.; Kephart, J.; Roland, C.; Bernholc, J. *Phys. Rev. Lett.* **2002**, *88*, 075506-1.
(7) Shimoda, H.; Gao, B.; Tang, X. P.; Kleinhammes, A.; Fleming, L.; Wu, Y.; Zhou, O. *Phys. Rev. Lett.* **2002**, *88*, 015502.
(8) Gao, B.; Bower, C.; Lorentzen, J. D.; Fleming, L.; Kleinhammes, A.; Tang, X. P.; McNeil, L. E.; Wu, Y.; Zhou, O. *Chem. Phys. Lett.* **2000**, *327*, 69.
(9) Zhao, J. J.; Buldum, A.; Han, J.; Lu, J. P. *Phys. Rev. Lett.* **2000**, *85*, 1706.
(10) Kar, T.; Pattanayak, J.; Scheiner, S. *J. Phys. Chem. A* **2001**, *105*, 10397.
(11) Liu, H. J.; Chan, C. T. *Solid State Commun.* **2003**, *125*, 77.

10.1021/cm048746+ CCC: $30.25
Published on Web 02/03/2005

proposed BC_3, BC_2N, and BN nanotube materials. The exploration of possible Li adsorption in these nanotubes, as well other inorganic nanostructured materials, is a worthy objective.[16,17]

The discovery of carbon nanotubes has opened many opportunities for obtaining novel one-dimensional nanostructured materials.[18] Many classes of nanotubes originating from hexagonal compounds, that is, BC_3, BN, and BC_2N, have been proposed and investigated.[19−28] The geometries and electronic properties of these nanotubes have been predicted theoretically, and the possibilities for technical applications have been proposed. While carbon nanotubes are well known to be either semiconducting or metallic, depending on their radii and chiralities,[29,30] BN nanotubes have an almost constant band gap (E_g) of 5.5 eV independent of their structures.[31] Recently, BN nanotubes are receiving much attention as candidates for high-capacity hydrogen storage.[32−34] Also, chiral BC_2N nanotubes might behave as nanoscale coils because of the anisotropic conductivity of the related sheets. This contrasts with the more isotropic carbon and BN nanotubes. BN, BC_3, and BC_2N nanotubes have been realized experimentally.[21−23,30,31] However, Li adsorption in these nanotubes has not been investigated experimentally or theoretically. We found recently that boron doping can improve the Li adsorption in SWNTs.[35] In the present investigation, lithium adsorption in C, BC_3, BC_2N, and BN SWNTs was simulated by density functional computations. The computed electronic structures and the Li adsorption energies of these doped SWNTs were compared. The predicted Li adsorption properties provide fundamental knowledge of Li intercalation in various nanotubes and should help direct experimental explorations of new nanostructured materials for possible Li ion battery applications.[36]

2. Computational Methods

2.1. Lithium Adsorption. Density function theory (DFT) based computations were performed with the generalized gradient approximation (GGA) proposed by Perdew et al.,[37] using a plane-wave pseudopotential CASTEP code.[38] The ultrasoft pseudopotentials proposed by Vanderbit were employed.[39] An energy cutoff for the plane waves of 400 eV was used along with periodically repeating tetragonal supercells with lattice constants *a*, *b*, and *c*.[40] Both *a* and *b* were chosen to ensure negligible interaction between the tube and its periodic images (the minimum C−C distance between two nearest neighboring tubes is taken to be over 10 Å). To avoid interaction between the adsorbed Li atoms and their periodic images along the tube axis, the typical computational supercell employed here includes two unit cells of the zigzag tube (a supercell with 64 atoms and supercell length $c = 8.43$ Å for pure C nanotube), or four unit cells of the armchair tube (a supercell with 96 atoms and supercell length $c = 9.76$ Å for pure C nanotube). Because of the very large supercell, only Γ point sampling of the reciprocal space was used for geometry optimization with the following convergence criteria: energy changes per atom less than 2×10^{-5} eV, the root-mean-square (RMS) of the forces less than 0.05 eV/Å, and the RMS displacement of atoms less than 2×10^{-3} Å. The positions of the first and the second nearest neighbor nanotube atoms away from the adsorbed Li were fully relaxed under the condition that the cell parameters and the coordinates of other atoms were fixed to the values optimized for the original tubes. Also, 6 or 10 k points were employed for sampling the one-dimensional Brillouin zone in the calculations of the zigzag and armchair nanotubes to obtain their adsorption energies, charge transfer, density of states (DOS), and band structures. Adsorption energies were computed for inner and outer Li adsorption sites of all of the nanotubes.

The Li adsorption energies measure the thermodynamic driving force for lithium adsorption on SWNTs and are defined here as the difference between the total energy of the complexed species (Li-host) and the sum of the energy of the separated host and the μ_{Li}, the energy per Li atom in bulk lithium metal used for lithium atom energy:

$$E_{adsorption} = E_{tot}(\text{Li-host}) - E_{tot}(\text{host}) - \mu_{Li} \quad (1)$$

It is important to note that the energy of a single Li atom computed at the level employed here is 1.85 eV higher than that of bulk lithium metal. This value is close to the heat of formation, 1.62 eV, of the lithium atom in the gas phase at 298.15 K. The GGA total energies of the fully optimized SWNT hosts (E_{tot}(host)) and

(12) Agrawal, B. K.; Agrawal, S.; Srivastava, R. *J. Phys.: Condens. Matter* **2004**, *16*, 1467.
(13) Cheng, H.; Cooper, A. C. *J. Mater. Chem.* **2004**, *14*, 715.
(14) Zhao, J. J.; Han, J.; Lu, J. P. *Phys. Rev. B* **2002**, *65*, 193401.
(15) (a) Xie, R. H.; Zhao, J. J.; Rao, Q. In *Encyclodedia of nanoscience and nanotechnology*; Nalwa, H. S., Ed.; American Scientific Publishers: CA, 2004; pp 2, 505. (b) Zhao, J. J.; Xie, R. H. *J. Nanosci. Nanotechnol*. **2003**, *3*, 459.
(16) Dominko, R.; Arcon, D.; Mrzel, A.; Zorko, A.; Cevc, P.; Venturini, P.; Gaberscek, M.; Remskar, M.; Mihailovic, D. *Adv. Mater.* **2002**, *14*, 1531.
(17) Gao, X. P.; Zhu, H. Y.; Pan, G. L.; Ye, S. H.; Lan, Y.; Wu, F.; Song, D. Y. *J. Phys. Chem. B* **2004**, *108*, 2868.
(18) Iijima, S. *Nature* **1991**, *354*, 56.
(19) Rubio, A.; Corkill, J. L.; Cohen, M. L. *Phys. Rev. B* **1994**, *49*, 5081.
(20) Miyamoto, Y.; Rubio, A.; Cohen, M. L.; Louie, S. G. *Phys. Rev. B* **1994**, *50*, 4976.
(21) Dillon, A. C.; Jones, K. M.; Bekkedahl, T. A.; Kiang, C. H.; Bethuune, D. S.; Heben, M. J. *Nature* **1997**, *386*, 377.
(22) Liu, C.; Fan, Y. Y.; Liu, M.; Cong, H. T.; Cheng, H. M.; Dresselhaus, M. S. *Science* **1999**, *286*, 1127.
(23) Bengu, E.; Marks, L. D. *Phys. Rev. Lett.* **2001**, *86*, 2385.
(24) Oku, T.; Kuno, M. *Diamond Relat. Mater.* **2003**, *12*, 840.
(25) Okada, S.; Saito, S.; Oshiyama, A. *Phys. Rev. B* **2002**, *65*, 165410.
(26) Xiang, H. J.; Yang, J. L.; Hou, J. G.; Zhu, Q. S. *Phys. Rev. B* **2003**, *68*, 035427.
(27) Kim, Y. H.; Chang, K. J.; Louie, S. G. *Phys. Rev. B* **2001**, *63*, 205408.
(28) Schmidt, T. M.; Baiele, R. J.; Piquini, P.; Fazzio, A. *Phys. Rev. B* **2003**, *67*, 113407.
(29) Saito, R.; Fujita, M.; Dresselhaus, G.; Dresselhaus, M. S. *Appl. Phys. Lett.* **1992**, *60*, 2240.
(30) Hamada, N.; Sawada, S.; Oshiyama, A. *Phys. Rev. Lett.* **1992**, *68*, 1579.
(31) Miyamoto, Y.; Rubio, A.; Louie, S. G.; Cohen, M. L. *Phys. Rev. B* **1994**, *50*, 18360.
(32) Ma, R. Z.; Bando, Y.; Zhu, H. W.; Sato, T.; Xu, C. L.; Wu, D. H. *J. Am. Chem. Soc.* **2002**, *124*, 7672.
(33) Tang, C. C.; Bando, Y.; Ding, X. X.; Qi, S. R.; Golberg, D. *J. Am. Chem. Soc.* **2002**, *124*, 14550.
(34) Wu, X. J.; Yang, J. L.; Hou, J. G.; Zhu, Q. S. *Phys. Rev. B* **2004**, *69*, 153411.
(35) (a) Zhou, Z.; Gao, X. P.; Yan, J.; Song, D. Y.; Morinaga, M. *J. Phys. Chem. B* **2004**, *109*, 9023. (b) Zhou, Z.; Gao, X. P.; Yan, J.; Song, D. Y.; Morinaga, M. *Carbon* **2004**, *42*, 2677.
(36) (a) Ceder, G.; Chiang, Y. M.; Sadoway, D. R.; Aydinol, M. K.; Jang, Y. I.; Huang, B. *Nature* **1998**, *392*, 694. (b) Liu, Y.; Fujiwara, T.; Yukawa, H.; Morinaga, M. *Electrochim. Acta* **2001**, *46*, 1151.
(37) Perdew, P.; Burke, K.; Wang, Y. *Phys. Rev. B* **1996**, *54*, 16533.
(38) Milman, V.; Winkler, B.; White, J. A.; Pickard, C. J.; Payne, M. C.; Akhmatskaya, E. V.; Nobes, R. H. *Int. J. Quantum Chem.* **2000**, *77*, 895.
(39) Vanderbilt, D. *Phys. Rev. B* **1990**, *41*, 7892.
(40) Dag, S.; Gulseren, O.; Yildirim, T.; Ciraci, S. *Phys. Rev. B* **2003**, *67*, 165424.

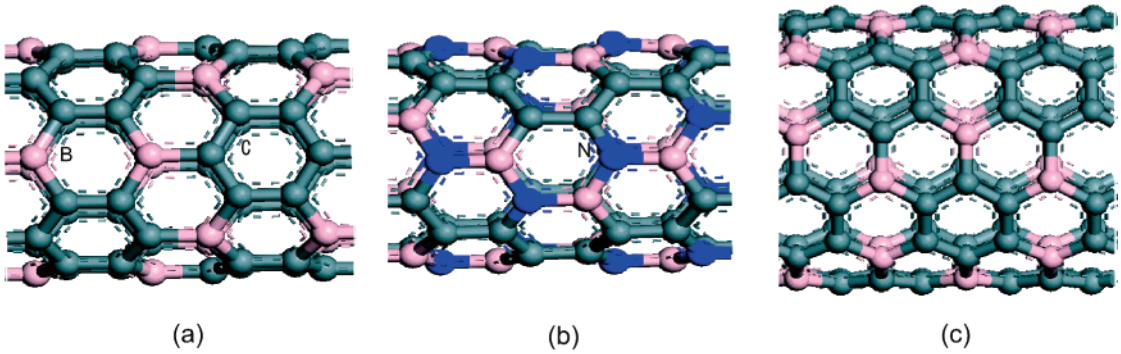

Figure 1. Typical structural models of various nanotubes used here: (a) the (4, 0) BC_3 nanotube, (b) the (4, 0) BC_2N nanotube, and (c) the (3, 3) BC_3 nanotube.

Table 1. Diameters *D*, Supercell Length *l*, and Average Bond Length *d* for Various Zigzag Nanotubes after Full Geometric Optimization

nanotube	D (Å)	l (Å)	d (Å)
(8, 0) C	6.29	8.43	$d_{C-C} = 1.41$
(4, 0) BC_3	6.54	8.85	$d_{C-C} = 1.41$, $d_{B-C} = 1.55$
(4, 0) BC_2N	6.40	8.57	$d_{C-C} = 1.41$, $d_{B-C} = 1.47$, $d_{N-C} = 1.35$, $d_{B-N} = 1.45$
(8, 0) BN	6.37	8.47	$d_{B-N} = 1.43$

the host with Li-adsorbed were employed in the evaluation of eq 1. By our definition, $E_{adsorption} < 0$ in eq 1 corresponds to exothermic chemical adsorptions leading to minima stable toward dissociation into the SWNT and bulk lithium. Endothermic energies, $E_{adsorption} > 0$, correspond to minima of adsorbed species which are unstable thermodynamically relative to the host model and bulk lithium. Species with $E_{adsorption} < 0$ are stable toward dissociation into the host and separated lithium atoms.

As BN nanotubes are known experimentally to adopt zigzag structures,[32,33] models for zigzag tubes (Figure 1) were computed and the results were compared. The structures of BN, BC_3, and BC_2N nanotubes can also be classified by the chirality notation (n, m) in analogy with C nanotubes.[31] BN (n, m) nanotubes are related to C (n, m) nanotubes. In contrast, the radii of BC_3 and BC_2N (n, m) nanotubes are comparable to those of the ($2m$, $2n$) C nanotubes.[20,31] (Note that the unit cells of BC_3 and BC_2N sheets are about 4 times larger than the unit cell of graphite.[31]) Although there are two types of BC_2N nanotubes,[20] only the more stable one (with more adjacent B and N atoms, Figure 1b) was investigated here. For comparison with the zigzag results, the Li adsorption in the armchair (6, 6) carbon and (3, 3) BC_3 nanotubes (Figure 1c) was also examined.

2.2. Li Diffusion. The entry pathway through a sidewall was modeled by moving a Li from an outer stable site above a ring gradually through the ring to the inner stable absorption site. This process employed fixed distances between the Li and the ring center; all of the neighboring atoms were fully relaxed at each Li distance. The diffusion barriers for Li through the sidewalls of C and BC_3 nanotubes were computed using the same procedure.

3. Results and Discussion

3.1. Optimized Structures of Undoped Nanotubes. The zigzag nanotubes with 64 atoms were fully relaxed in supercells, and the optimized structures are shown in Table 1. Reflecting the bond lengths in borazene and benzene, the B−N bond in (8, 0) BN nanotubes (1.43 Å) is slightly longer than the C−C bond in the pure (8, 0) carbon nanotube (1.41 Å). In line with the covalent atomic radii, the bond length relationships in the other nanotubes are BC > CC > NC. The BC bonds are shorter in the (4, 0) BC_2N than in the (4, 0) BC_3 nanotube, because the former has more electrons. As a consequence of these individual bond lengths, the diameter, D, and the tubule length, l, are largest in the BC_3 nanotubes, intermediate in the (4, 0) BC_2N and BN nanotubes, and smallest in the pure (8, 0) nanotube (Table 1).

3.2. Lithium Adsorption Energies. The structures and Li adsorption energies for various nanotubes are given in Figure 2. Most importantly, the Li adsorption energies of the (4, 0) BC_3 nanotubes at both inner and outer sites (in the −0.44 to −0.58 eV range) are much more favorable than the (8, 0) carbon nanotubes (range 0.03 to −0.09 eV). The computed energies for Li adsorption at both inner and outer sites of the two types of six-membered rings (6MR) in BC_3 tubes (labeled 1 and 2 in Figure 2) are all large, negative, and nearly the same. Because of this independence of the adsorption sites and the relative location of B atoms on the tube sidewall, Li's should move rather freely along the entire exterior and interior of the BC_3 nanotubes.

However, the Li adsorption energies in (8, 0) BN nanotubes are highly positive (1.58−2.00 eV based on bulk lithium, eq 1), indicating that Li adsorption is not feasible energetically. When the Li atom is forced to occupy locations directly above a boron or a nitrogen atom, the adsorption energies (1.93 eV (B) and 2.00 eV (N)) are even larger than those with Li above a 6MR center. It is obvious that BN nanotubes are not attractive candidates for Li intercalated material applications, even though BN nanotubes are promising hydrogen storage media.[31,32,40]

Li adsorption in (4, 0) BC_2N nanotubes is more complicated, because there are three anisotropic sidewall Li adsorption sites (labeled 1−3 in Figure 2) and all have quite different adsorption energies. The most favorable site (and the only one with a negative adsorption energy) is outside, above the 6MR with 4 carbon atoms (position 3). As discussed in the following section, the differences in the Li adsorption energies in various nanotubes are strongly related to their electronic structures.

The Li adsorption energies for armchair (6, 6) C and (3, 3) BC_3 nanotubes, with Li adsorbed at both inner and outer sites, are larger in magnitude than their zigzag counterparts (Figure 2). The Li adsorption energy in the (6, 6) C nanotube is about 0.59 eV (inner) and 0.78 eV (outer), while the Li adsorption energies in the (3, 3) BC_3 nanotube range from −0.80 to −0.89 eV at the four different adsorption sites. The difference in the Li adsorption energies in armchair (6,

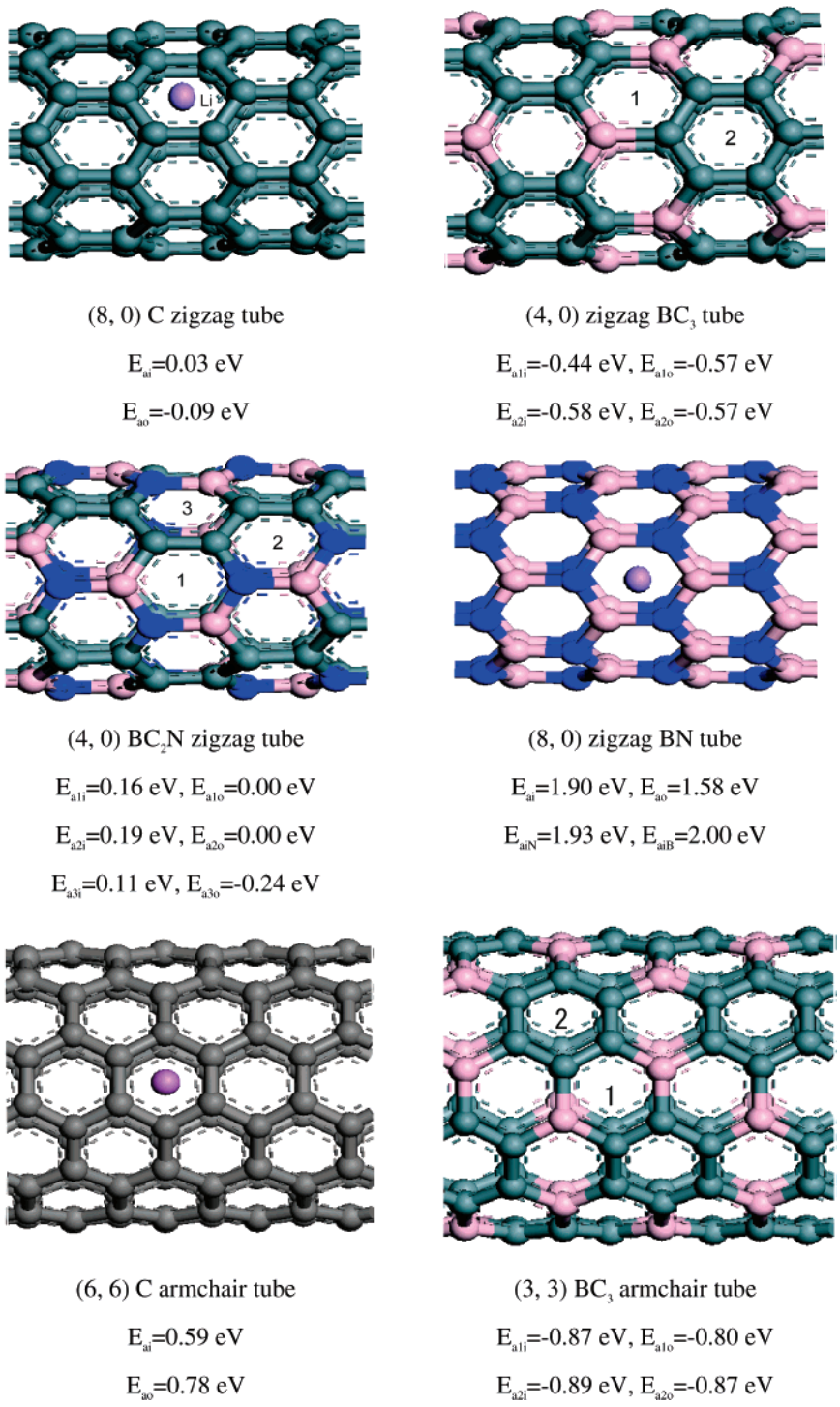

Figure 2. Li adsorption energies in various nanotubes. E_{ai} denotes the adsorption energy of Li located at the inner site, and E_{ao} denotes the adsorption energy of Li located at the outer site. For BN nanotubes, E_{aiN} and E_{aiB} denote the adsorption energy of Li located above the N atom and the B atom inside the tube, respectively.

6) C and (3, 3) BC_3 is much larger than in zigzag (8, 0) C and (4, 0) BC_3 nanotubes. Both zigzag and armchair BC_3 nanotubes adsorb Li very well thermodynamically.

The Li adsorption energies of BC_3 nanotubes are more negative than those in the pure C nanotubes both at inner and at outer sites; therefore, the BC_3 nanotubes have energetically more favorable sites for additional Li adsorption. When two adsorbed Li atoms inside (8, 0) C or (4, 0) BC_3 zigzag nanotubes are included in one computational supercell, the Li atoms, after full relaxation, are located beneath two neighboring 6MR's. The computed average Li adsorption energies per Li atom were 0.44 eV for the (8, 0) C and −0.21 eV for the (4, 0) BC_3 nanotubes. For the pure (8, 0) C tube, the adsorption energy (E_a) for the first Li atom is 0.03 eV (Figure 2), while the adsorption energy for the second Li atom is highly endothermic, 0.85 eV. This indicates that the step-by-step adsorption mechanism is not feasible for pure carbon tubes. The high capacity of Li storage in C tubes (maximum of $Li_{2.7}C_6$)[7,8] may be due to formation of Li_2^+ or small ionized Li_n clusters (see below). In contrast, the energy of the second Li adsorption in the (4, 0) BC_3 tube, although endothermic, is reduced much less

Table 2. Changes in Net Charges of B, C, and N in Different Nanotubes before and after Li Adsorption at Inner Sites[a]

	C		B		N	
	before	after	before	after	before	after
(8, 0) C nanotube	0	−0.15				
(6, 6) C nanotube	0	−0.16				
(4, 0) BC_3 nanotube	−0.20	−0.30	0.60	0.31		
(3, 3) BC_3 nanotube	−0.20	−0.33	0.60	0.31		
(8, 0) BN nanotube			0.87	0.65	−0.87	−0.83

[a] The net charge after Li adsorption is the average of the first neighboring atoms of adsorbed Li.

than in the (8, 0) C nanotubes. When the first Li is inside site 1, the energy of the second Li attachment is +0.02 eV. When the first Li is located inside site 2, the energy of the second Li attachment is +0.16 eV (see Figure 2). The overall negative adsorption energies for the attachment of two Li's clearly predict that the Li storage capability of the BC_3 nanotubes should be greater than for C nanotubes.

3.3. Changes in Net Charges of Nanotubes after Li Adsorption. During adsorption, Li atoms transfer electrons to the nanotubes. Due to the electrostatic interaction, the resulting Li^+ cations "localize" the negative charge to nearby atoms on the tube sidewall.[6,9] Changes in net charges of B, C, and N in different nanotubes before and after Li adsorption at inner sites are summarized in Table 2. Note that the net charges after Li adsorption are the average values of the first set of atoms neighboring the adsorbed Li. In both zigzag and armchair BC_3 nanotubes, the boron charges are much less positive after Li adsorption, indicating that B atoms accept the electron density more effectively than carbon. Lithium adsorption partially alleviates the electron deficiency of these boron-rich nanotubes. This contributes to their stability. In contrast, the carbon atoms only become −0.15 to −0.16 more negative in the C nanotubes. These tubes are "electron sufficient", and the extra electron density from lithium does not improve the bonding. Likewise, in the electron-sufficient BN nanotubes, only the borons (rather than the much more electronegative but already highly negatively charged nitrogen atoms) accept electron density after lithium adsorption. The highly unfavorable Li adsorption energies in BN nanotubes are a consequence.

3.4. Electronic Structures of C, BC_3, and BN Nanotubes. The band structures for C, BC_3, and BN nanotubes are shown in Figure 3. Figure 4 displays the density of states (DOS) and partial density of states (PDOS) for the (4, 0) BC_3 and the (8, 0) BN nanotubes. The (8, 0) C nanotube is a well-known semiconductor (see Figure 3a); our computed GGA band gap is $E_g \approx 0.71$ eV. The (4, 0) BC_3 nanotube is also a semiconductor according to our computations (see Figure 3b). Its band gap, $E_g \approx 0.66$ eV, smaller than that of the (8, 0) C nanotubes, is close to a previous result (0.6 eV).[27] The BC_3 nanotube DOS (Figure 4a) shows that carbon contributes more than boron to the valence band, but that both elements contribute almost equally to the conduction band. Indeed, the B−C bonds have partial ionic character in BC_3 nanotubes: the charges are +0.6 on B and −0.2 on C (Table 2). All of the C atoms in pure carbon nanotubes bond covalently and form conjugated 6MRs. As mentioned above, BN nanotubes are semiconductors; the width of their band gaps ($E_g \approx 5.5$ eV) is almost independent of their diameter, helicity, and even the number of tube sidewalls.[20]

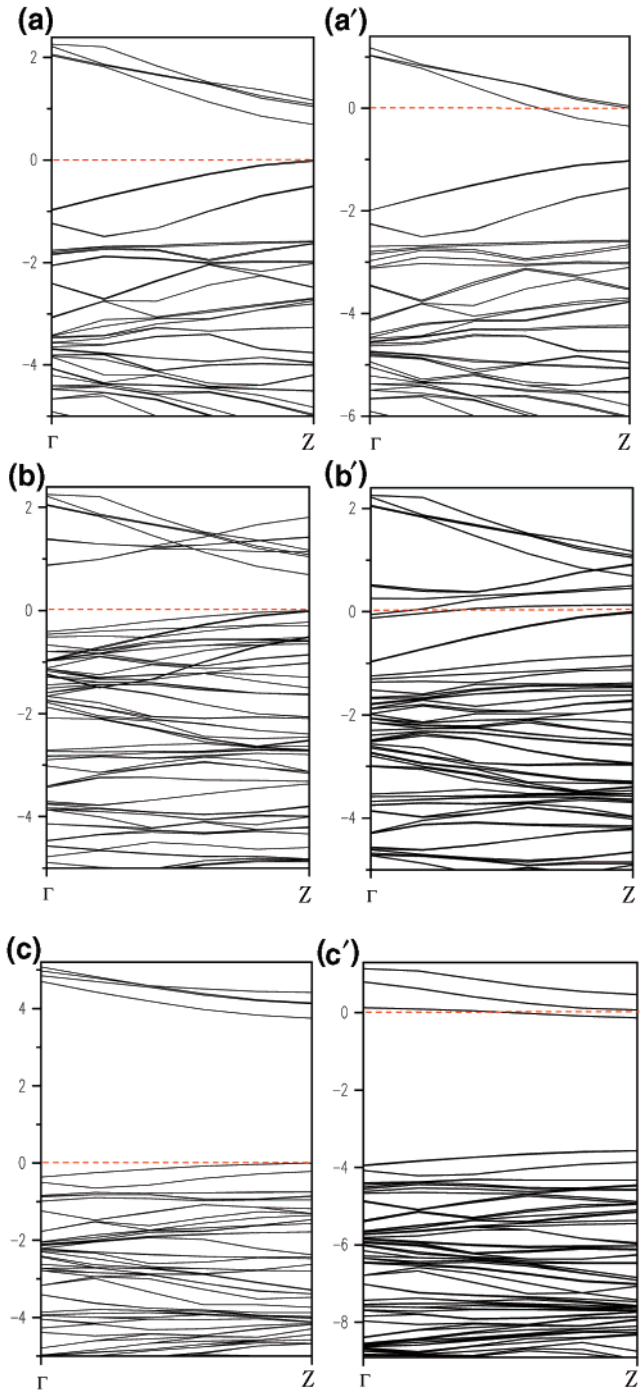

Figure 3. Band structures for (a) (8, 0) carbon nanotube, (b) (4, 0) BC_3 nanotube, and (c) (8, 0) BN nanotubes, and for (a′) (8, 0) carbon nanotube, (b′) (4, 0) BC_3 nanotube, and (c′) (8, 0) BN nanotubes after Li is adsorbed at the inner site 1 as described in Figure 2. The dashed lines denote Fermi level.

Figure 3c shows that the (8, 0) BN nanotube has the typical band structure of wide band gap semiconductors. The

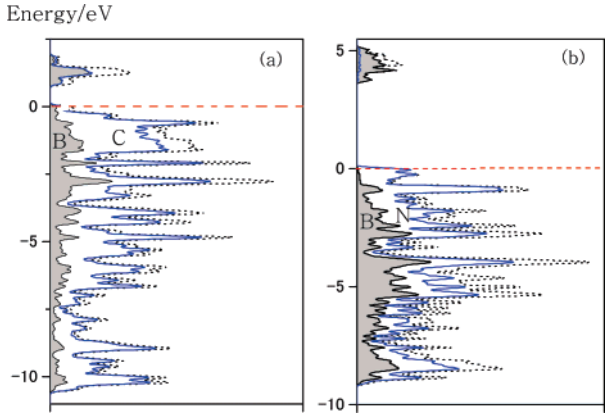

Figure 4. Density of states (DOS) and partial density of states (PDOS) for (a) (4, 0) BC_3 nanotube and (b) (8, 0) BN nanotubes. The dashed lines denote Fermi level.

calculated GGA band gap, $E_g \approx 3.66$ eV, is very close to the previous result, 3.65 eV.[34] While the N component contributes more to the valence band of BN nanotubes, boron dominates the conduction band composition (see Figure 4b). As expected from the difference in element electronegativities, the bonding in BN nanotubes is more ionic; the charges are B +0.87 and N −0.87 (Table 2).

The band structures for Li-adsorbed C, BC_3, and BN nanotubes also are shown in Figure 3. After Li adsorption, the Fermi level in all of the above three nanotubes shifts into the conduction band. Although (8, 0) C as well as (4, 0) BC_3 nanotubes are semiconductors and (8, 0) BN nanotube is wide-band-gap semiconductor, all three are transformed into metals after Li adsorption. The band structures of the (8, 0) C and BN nanotubes are not modified significantly by the Li adsorption; most of the bands resemble those of undoped tubes (in agreement with ref 9). Li adsorption modifies the band structure of BC_3 nanotubes, due to the strong interaction between the adsorbed Li and the BC_3 nanotube host. Thus, the Li adsorption energies in BC_3 nanotubes have large negative values, as we have found.

Note that all carbon and BN nanotubes are isoelectronic and electron sufficient, but that the BC_3 and other boron-doped nanotubes are electron deficient. The donation of electrons from lithium atoms alleviates this electron deficiency, which explains the favorable adsorption energetics.

The electron density contour plots of the nanotubes are shown in Figure 5; the slices are through the tube sidewalls. As no noticeable changes are apparent after Li adsorption, these contour plots are not presented. The conjugated 6 MR electronic structure of the carbon nanotube is seen clearly. The BC_3 nanotube also shows this feature, but the electron density near the B atoms is lower. As discussed above, adsorbed Li atoms transfer electrons to the nanotubes, and the negative charges will be distributed mainly among the more electronegative neighboring C atoms in the tube sidewall. The electron-deficient BC_3 nanotubes accept electrons from the adsorbed Li atom effectively. Typically, the C−C covalent bonds are stretched and weakened due to Li adsorption,[41] but the presence of B reduces such effects.[35]

(41) Liu, Y.; Yukawa, H.; Morinaga, M. *Comput. Mater. Sci.* **2004**, *30*, 50−56.

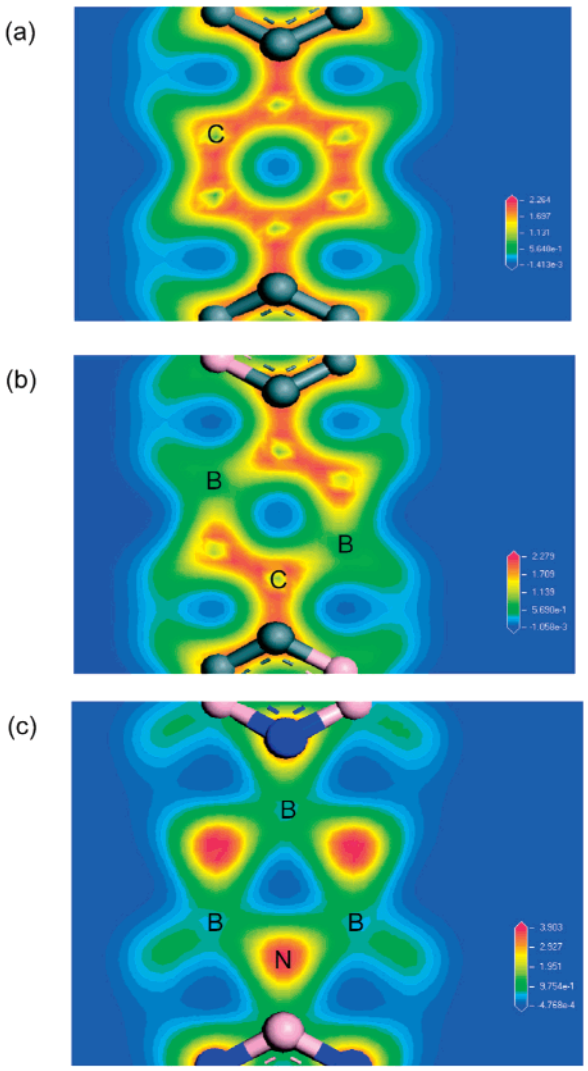

Figure 5. Contour plots for the electron density on a slice through the wall of C (a), BC_3 (b), and BN (c) zigzag nanotubes.

In general, the electron-deficient B 6MR's are stabilized by additional electrons, resulting in the large negative values for Li adsorption energies in BC_3 nanotubes. In Figure 5c, the electrons in the BN nanotube are localized at N atoms, and B−N bonds have more ionic character. Lithium, if adsorbed on the tube sidewalls, cannot transfer electron density to the tube effectively due to the electron-sufficient ionic bonding of BN nanotubes (Table 2). Consequently, BN nanotubes have very large positive adsorption energies and are unsuitable for Li intercalation. In addition, BN nanotubes have wide band gaps and exhibit lower electrical conductivity, which restricts Li ion battery applications.

The band structures for armchair carbon and BC_3 nanotubes are presented in Figure 6. Although the (6, 6) carbon nanotube is metallic, the (3, 3) BC_3 nanotube is found to be a semiconductor due to the presence of B, as shown in Figure 6b. The band gap of the (3, 3) BC_3 nanotube, E_g, is calculated to be about 0.45 eV. Analogous to armchair nanotubes, Li adsorption shifts the Fermi level into the conduction band in both nanotubes. Yet the modification of BC_3 nanotube band structures by Li adsorption is more pronounced.

Thus, the electronic character of nanotubes affects the lithium storage performance critically. The electron-deficient

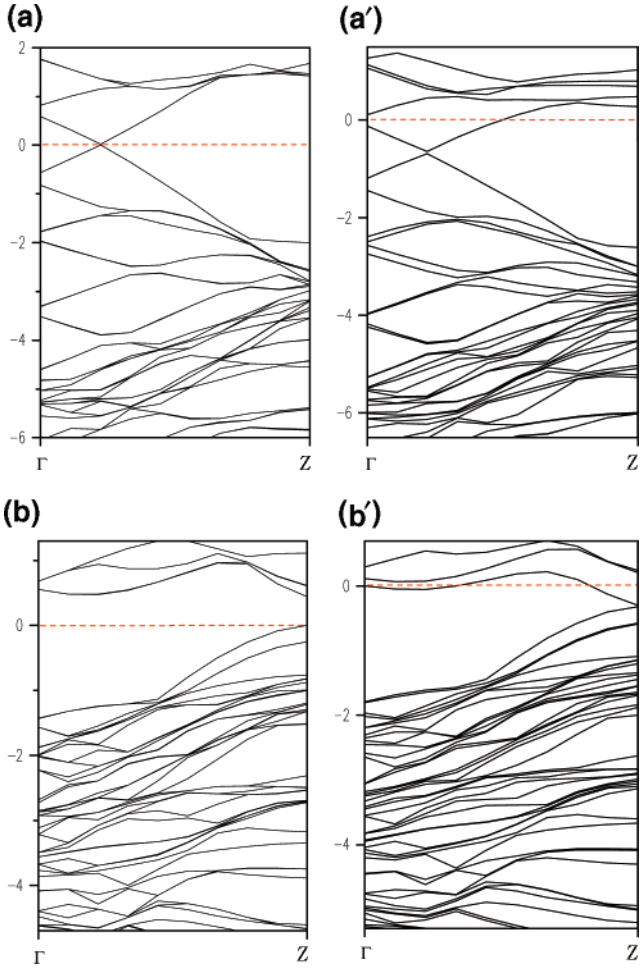

Figure 6. Band structures for (a) (6, 6) carbon nanotube and (b) (3, 3) BC_3 nanotube, and (a′) (6, 6) carbon nanotube and (b′) (3, 3) BC_3 nanotube after Li is adsorbed at inner site. The dashed lines denote Fermi level.

B-doped forms of C nanotubes should adsorb lithium effectively, whereas the localized nonaromatic BN tubes should not. The elasticity is less important than the electronic factor for Li adsorption in the nanotubes under consideration. There is no direct correlation between the lithium adsorption energies and the elasticity of the carbon and composite nanotubes: the carbon nanotubes are stiffer than BC_3, BC_2N, and BN tubes,[42] although BC_3 is the best prospect to store lithium thermodynamically.

3.5. Computations in Small Models. The critical influence of the electronic character of nanotubes on the lithium storage performance can also be seen from the small model studies. While the binding energies between atomic Li and benzene or C_4BNH_6 are relatively small, −0.23 and −0.62 eV at B3LYP/6-311+G** with zero point energy correction, respectively (computations were performed using the Gaussian 98 program[43]), the binding energy is dramatically large, −2.65 eV, for binding of a Li atom to the electron-deficient $C_4B_2H_6$ (Scheme 1). In contrast, a lithium atom does not bind to borazene[44] favorably at all.

Moreover, the dilithium molecule Li_2 binds 0.42 eV more strongly to one side of benzene than the sum of two individual Li atom attachments above and below the benzene ring. Ring bending (**2**, Scheme 1), as in the real nanotube systems, results. Isomer **2** has a much larger HOMO−LUMO energy difference (2.78 eV for **2** vs 1.83 eV for **3**).

To gain more chemical insight into the electron delocalization of these two isomers, canonical molecular orbital (CMO) dissected[45] nucleus independent chemical shifts (NICS)[46] analyses have been performed. NICS,[46] a simple and efficient aromaticity probe, is the negative of the magnetic shielding computed at chosen points in the vicinity of molecules. Significantly negative (i.e., magnetically shielded) NICS values in interior positions of rings or cages indicate the presence of induced diatropic ring currents or "aromaticity", whereas positive values (i.e., deshielded) at each points denote paratropic ring currents and "antiaromaticity". CMO NICS analysis[45] dissects the total NICS value to give the individual contributions from each canonical molecular orbital. The computed total π-like NICS at ring centers (nonweighted mean of the ring carbon atoms) for **2** and **3** are −2.2 and 12.9 ppm, respectively, indicating that **2** is π nonaromatic, while **3** is π antiaromatic. The large difference between the HOMO contributions (5.9 ppm in **2** vs 24.9 ppm in **3**) (Figure 7) is due to the differences in HOMO−LUMO gap energies between **2** and **3** and accounts for their significantly different aromatic character. Note that both the boat form benzene dianion as in bis[(tetrahydrofuran)lithium(I)] hexakis(trimethylsilyl)benzenide[47] and the planar 6-center 8 π antiaromatic benzene dianion as in bis[(dimethoxyethane)lithium(I)]1,2,4,5-Tetrakis(trimethylsilyl)benzenide[48] were successfully synthesized. The substituents and the ligands are important in stabilizing the planar 6C-8 π antiaromatic benzene dianion.[48]

Li_2 also binds to the BN doped benzene ring (**6** and **7** in Scheme 1), but the isomer **5** with two separate lithium atoms is lower in energy.

Although Li_2 binds strongly to the face of $C_4B_2H_6$, its isomer with individual Li atoms on opposite sides (**9**, Scheme 1) is even more favorable. In both cases, the 4π antiaromatic $C_4B_2H_6$ is converted to 6π aromatic $C_4B_2H_6Li_2$.

Thus, it is possible that dilithium can be adsorbed favorably on the exterior of carbon nanotubes and BC_2N

(42) Hernández, E.; Goze, C.; Bernier, P.; Rubio, A. *Phys. Rev. Lett.* **1998**, *80*, 4502.
(43) Frisch, M. J.; Trucks, G. W.; Schlegel, H. B.; Scuseria, G. E.; Robb, M. A.; Cheeseman, J. R.; Zakrzewski, V. G.; Montgomery, J. A., Jr.; Stratmann, R. E.; Burant, J. C.; Dapprich, S.; Millam, J. M.; Daniels, A. D.; Kudin, K. N.; Strain, M. C.; Farkas, O.; Tomasi, J.; Barone, V.; Cossi, M.; Cammi, R.; Mennucci, B.; Pomelli, C.; Adamo, C.; Clifford, S.; Ochterski, J.; Petersson, G. A.; Ayala, P. Y.; Cui, Q.; Morokuma, K.; Malick, D. K.; Rabuck, A. D.; Raghavachari, K.; Foresman, J. B.; Cioslowski, J.; Ortiz, J. V.; Stefanov, B. B.; Liu, G.; Liashenko, A.; Piskorz, P.; Komaromi, I.; Gomperts, R.; Martin, R. L.; Fox, D. J.; Keith, T.; Al-Laham, M. A.; Peng, C. Y.; Nanayakkara, A.; Gonzalez, C.; Challacombe, M.; Gill, P. M. W.; Johnson, B. G.; Chen, W.; Wong, M. W.; Andres, J. L.; Head-Gordon, M.; Replogle, E. S.; Pople, J. A. *Gaussian 98*; Gaussian, Inc.: Pittsburgh, PA, 1998.
(44) Schleyer, P. v. R.; Jiao, H.; Hommes, N. J. R. v. E.; Malkin, M. G.; Malkina, O. *J. Am. Chem. Soc.* **1997**, *119*, 12669.
(45) (a) Corminboeuf, C.; Heine, T.; Weber, J. *Phem. Chem. Chem. Phys.* **2003**, *5*, 246; *J. Phys. Chem. A* **2003**, *107*, 6470. (b) Corminboeuf, C.; Heine, T.; Seifert, G.; Schleyer, P. v. R.; Weber, J. *Phys. Chem. Chem. Phys.* **2004**, *6*, 273.
(46) Schleyer, P. v. R.; Maerker, C.; Dransfeld, A.; Jiao, H.; Hommes, N. J. R. V. E. *J. Am. Chem. Soc.* **1996**, *118*, 6317.
(47) Sekiguchi, A.; Ebata, K.; Kabuto, C.; Sakurai, H. *J. Am. Chem. Soc.* **1991**, *113*, 1464.
(48) Sekiguchi, A.; Ebata, K.; Kabuto, C.; Sakurai, H. *J. Am. Chem. Soc.* **1991**, *113*, 1464.

Scheme 1. Optimized Structures and the Binding Energies (BE) of Some Lithium Complexes[a]

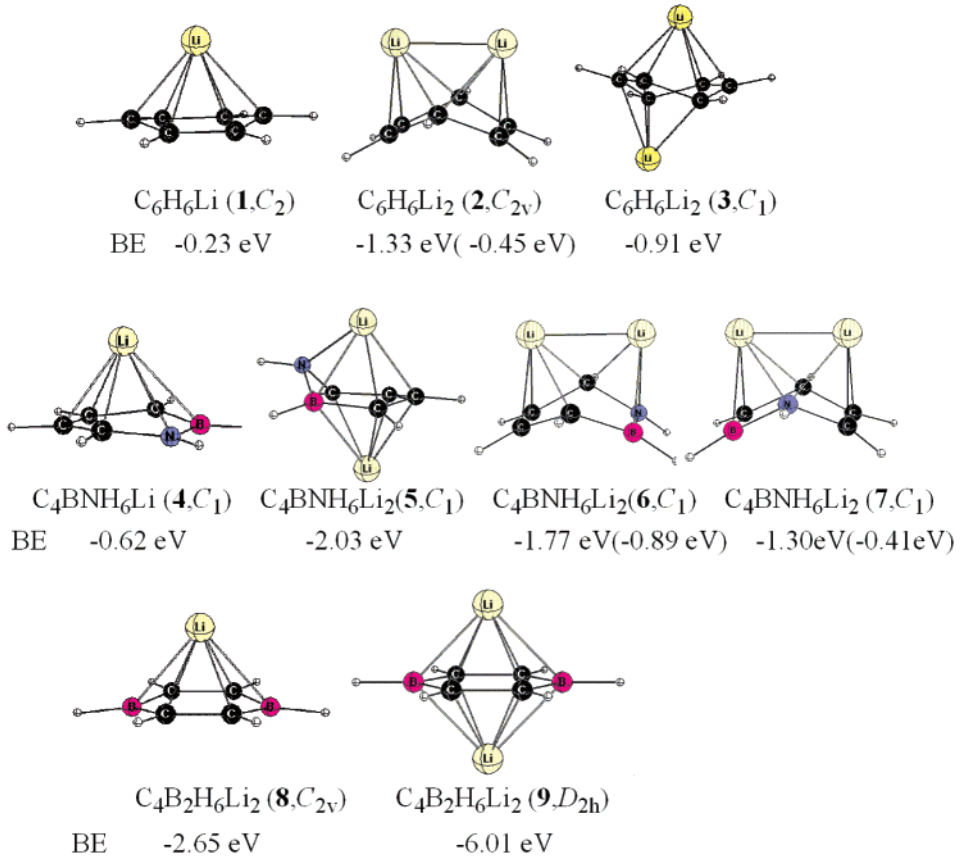

[a] The BE values given in the parentheses are those obtained relative to the ring molecule and dilithium molecule.

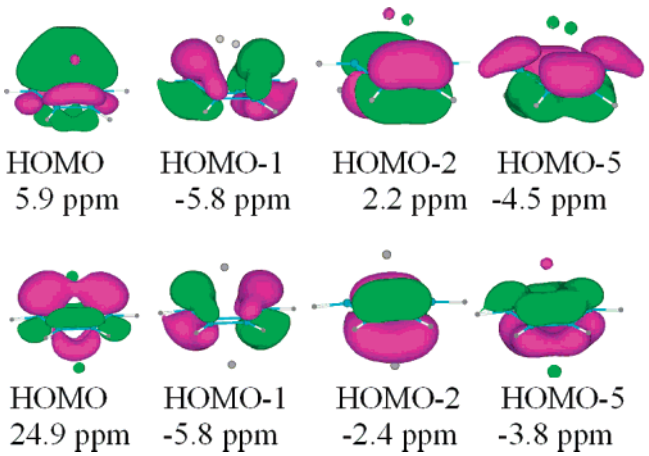

Figure 7. CMO NICS of the π-like orbitals in **2** and **3** of Scheme 1.

tubes, while the BC_3 tubes can adsorb lithium atoms both inside and outside. Further studies using PBC computations are in progress.

3.6. Diffusion Paths of Li in C and BC_3 Nanotubes. Information about the diffusion path also is important to understand the Li intercalation process.[6,10] We investigated the Li diffusion behavior in nanotubes by evaluating different diffusion channels. The energy difference when Li is located at the most stable site and then at the saddle point is defined as the barrier. As the true saddle point is very difficult to locate precisely, it was assumed to be the midpoint of the line connecting two stable Li adsorption sites.[49] The energy barrier for Li diffusion inside (8, 0) C nanotubes is calculated by this approximate (but adequate) method to be about 0.11 eV, close to the value reported by Meunier et al.[6] Similarly, the computed energy barrier for diffusion inside (4, 0) BC_3 nanotubes is about 0.08 eV. These low energy barriers confirm the expectation that Li diffusion in the interior of both C and BC_3 nanotubes is quite facile. Thus, the key problem is how Li enters the interior of nanotubes.

Previous theoretical investigations showed that the Li cannot penetrate the perfect sidewalls of pure nanotubes because the energy barriers are too large. Alternatively, Li can enter the tubes through topological defects and open ends.[6,10] The presence of B atoms in tube sidewalls influences the entry of Li into the tube interior strongly. We simulated this process by moving Li from the outer site gradually to the inner Li adsorption site. The results are shown in Figure 8 for (8, 0) carbon and for (4, 0) BC_3 nanotubes. The energy barrier for the carbon nanotube is about 9.5 eV, close to Meunier et al.'s result.[6] However, the barrier for lithium passage through the wall of (4, 0) BC_3 nanotubes (the 6MR labeled 2 in Figure 2) is only half as large (about 4.6 eV). Although the presence of B in the wall decreases the energy barrier dramatically, it is still too high for Li to enter through perfect sidewalls. Obviously, Li entry into the tube is dominated by steric effects, even though the electronic structure has a pronounced influence. Li only can enter the interior of tubes through topological defects and open ends. Li intercalation in nanotubes would be facilitated by experi-

(49) Koyama, Y.; Yamada, Y.; Tanaka, I.; Nishitani, S. R.; Adachi, H.; Murayama, M.; Kanno, R. *Mater. Trans.* **2002**, *43*, 1460.

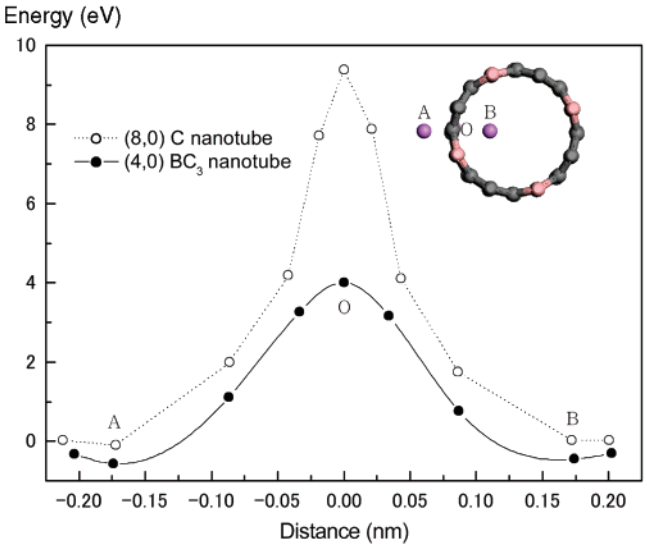

Figure 8. Energetics of diffusion pathways for Li ion passing through the sidewall of a (8, 0) C nanotube and a (4, 0) BC_3 nanotube. A, B, and O denote the two adsorption sites and the saddle point on the diffusion path, respectively.

mental methods which create open ends or more defects on the tube sidewalls.[7,8] We expect the combination of structural defects and doping by B impurity to reduce the energy barrier for Li entry into the tube interior further. Simulations exploring this are underway.

Mukhopadhyay et al.[50] investigated the electrochemical Li insertion in B-doped MWCNT, but we are not aware of any experimental reports on Li adsorption in BC_3 nanotubes. Experimental studies of Li intercalation in BC_3 nanotubes and in nanotubes with even higher B ratios should be rewarding.

4. Conclusions

According to the density functional computations, both zigzag and armchair BC_3 nanotubes have large Li adsorption energies, particularly at the preferred Li adsorption sites. In contrast, Li adsorption in (8, 0) BN nanotubes is unfavorable energetically. The behavior of BC_2N nanotubes is more complicated; the Li adsorption energies at different sites vary.

The electronic structure is vital for the Li adsorption in various nanotubes. BC_3 nanotubes are electron deficient, in contrast to the electron-sufficient C nanotubes. In both zigzag and armchair BC_3 nanotubes, the boron net charges are less positive after Li adsorption, indicating that B atoms accept electron density from the adsorbed Li atoms. Consequently, Li adsorption in the BC_3 tubes is favorable. The ionic character of the bonding is considerable in (8, 0) BN nanotubes, resulting in very unfavorable lithium adsorption energies. Also, wide-band-gap BN nanotube semiconductors have low electrical conductivity and thus are not suitable for Li ion battery applications.

The energy barrier is about 9.5 eV for the lithium atom penetration of a six-membered ring of (8, 0) carbon nanotubes; the barrier is much less, about 4.6 eV, for (4, 0) BC_3 nanotubes. However, the latter energy barrier is still too high for Li to enter the tube through perfect sidewalls. Nevertheless, the combination of topological defects and B impurities on nanotube sidewalls is expected to decrease the energy barrier for Li entry into the tube interior. The Li atoms may also enter through open ends. BC_3 nanotubes are prospective intercalation materials in Li ion battery applications.

Model studies show that it is possible that dilithium can be adsorbed favorably on the exterior of carbon nanotubes and BC_2N tubes, while the BC_3 tubes can adsorb lithium atoms both inside and outside. This may lead to even higher lithium storage ability for the BC_3 nanotubes. Further studies are in progress.

Acknowledgment. This study was supported by a Grant-in-Aid for Scientific Research from the Ministry of Education, Culture, Sports, Science, and Technology of Japan, by the 973 program (2002CB211800) in China, and by NSF Grant CHE-0209857 in the USA. Z.C. thanks the Alexander von Humboldt Foundation for supporting the summer visit in Germany.

CM048746+

(50) Mukhopadhyay, I.; Hoshino, N.; Kawasaki, S.; Okino, F.; Hsu, W. K.; Touhara, H. *J. Electrochem. Soc.* **2002**, *49*, A39.